PHYSICAL REVIEW VOLUME 169, NUMBER 5 25 MAY 1968

Determination of the Nucleon-Nucleon Scattering Matrix. VIII. (p,p) Analysis from 350 to 750 MeV*

MALCOLM H. MACGREGOR, RICHARD A. ARNDT,† AND ROBERT M. WRIGHT
Lawrence Radiation Laboratory, University of California, Livermore, California
(Received 13 November 1967)

All of the available (p,p) data from 350 to 750 MeV have been analyzed together with matrix representations for the data at lower energies. Several energy-dependent forms for the phase shifts were investigated, including forms using contributions from σ, ρ, and ω resonances. The most useful form, form A with 31 free parameters, gave a least-squares value $\chi^2=1575$ for a fit to data and matrices representing 1147 individual data from 23 to 736 MeV. Several different methods of including the inelastic scattering effects were studied. Although the inelastic scattering has an important effect on the elastic phases, an analysis of the elastic scattering data gives little information about the inelastic phases. A single-energy analysis at 425 MeV, where inelastic effects are very small, gave a well-defined result. However, a similar analysis at 630 MeV, where the total inelastic cross section is almost as large as the total elastic cross section, gave only qualitatively correct values for S, P, and D phases, and gave little information about the F and higher phases. The (p,p) elastic scattering matrix can now be defined accurately at energies from 0 to 450 MeV, but at energies above 450 MeV more experimental and theoretical information is still needed before a reliable analysis can be carried out.

I. INTRODUCTION

IN paper VII of this series,[1] we published a phase-shift analysis of the (p,p) scattering data below 400 MeV. In the present paper, we give the corresponding phase-shift analysis of the (p,p) scattering data above 400 MeV. The analyses in these two papers are not on the same footing for the following reasons: (a) At energies below 400 MeV, inelastic effects are very small and, in fact, can be ignored, as was done in VII. However, at energies above 400 MeV, the inelastic effects must in some manner be included. At 660 MeV, almost half of the scattering events are inelastic. (b) At low energies only a few partial waves contribute significantly to the scattering, and the rest can be calculated from theory. At the higher energies, all phases up through at least H waves must be treated phenomenologically. (c) At a number of energies below 400 MeV, reasonably complete sets of elastic scattering data exist. However, at energies above 400 MeV, extensive elastic scattering data sets exist only at two energies, 425 and 630 MeV. Neither of these data sets is as complete as are some of the lower-energy data sets, although the situation is improving rapidly. However, the inelastic data that must be analyzed together with the elastic data at these higher energies are very meager, and theoretical models used to reproduce the inelastic scattering results are very crude. At energies other than the narrow bands centered at 425 and 630 MeV, only scattered (p,p) measurements of various kinds exist.

For the above reasons, our handling of the phase-shift analysis is quite different in the present paper than it was in VII. In VII we made a very careful data selection, choosing only the data that gave a self-consistent set. We then examined a number of different phase-shift energy-dependent forms to obtain the one that gave the best fit with the smallest number of free parameters. A single unique solution exists in the elastic energy region, and we only studied minor variations in the form of that solution. In the present paper, we have kept essentially all of the available data except for a few points that we are certain must be incorrect. Many of the data sets are fit quite poorly, but since we have neither the reliable reference data set nor the well-founded phase-shift energy forms that we had at the low energies, we have little basis on which to select among the various data sets. We have tried a number of different forms for the phase-shift energy dependence, and these results are given here. But a well-defined unique solution for the elastic scattering does not really exist at energies much above 400 MeV, and we can tell very little from experiment about the behavior of the inelastic scattering amplitudes.

As in VII, we have contacted many experimentalists and have obtained essentially all of the data between 400 and 750 MeV that were in existence as of July 1967. Perhaps the most useful part of the present analysis is as a guideline in planning future experiments. We can also make some statements about the consistency of the existing data.

Since the phase-shift solutions are only qualitative, at least above 425 MeV, we have not tried to calculate corridors of errors for the various energy-dependent solutions. The scatter among the solution values indicates the uncertainties. In the single-energy analyses at 425 MeV, the phase-shift errors as deduced from the error matrix seem to have some meaning. However, at 630 MeV the quoted phase-shift errors are clearly misleading. The χ^2 surface in parameter space at this energy is not even approximately parabolic.

In Sec. II, we describe the data selection. Section III is a discussion of the treatment of the inelasticity.

* Work performed under the auspices of the U. S. Atomic Energy Commission.
† Present address: Virginia Polytechnic Institute, Blacksburg, Va.
[1] M. H. MacGregor, R. A. Arndt, and R. M. Wright, preceding paper, Phys. Rev. 169, 1128 (1968).

Section IV gives the results of the energy-dependent analyses, and Sec. V gives the results of the energy-independent analyses. Section VI summarizes our conclusions.

The analysis in the present paper is actually an analysis from 0 to 750 MeV, but the energy range given in the title was chosen so that the reader would not conclude that the present results for the lower energies supersede the results from paper VII.

II. DATA SELECTION

The data that we have considered for the present analysis are listed in Table I. References to these data are given in Table II. Since the analysis of (p,p) data above 400 MeV should obviously be correlated with the analysis below 400 MeV, we have made a data selection that extends essentially from 0 to 750 MeV. Because of the large number of data involved, about 1400 in all, we did not include the low-energy data (below 350 MeV) directly. Instead, we used matrix representations of the sets of data at 25, 50, 95, 142, 210, and 330 MeV (they are given in Table VII of paper VII). As we have shown in paper VII, a fit to the matrix representation of the data is essentially equivalent to fitting the data directly. The six matrices listed in Table I contain most of the physical content of the complete 0–400-MeV data selection, as was also demonstrated in paper VII. The data from 358 to 400 MeV are included both in paper VII and in the present work. A comparison between the results in the two cases gives a measure of the consistency of the two types of analysis.

A total of 599 data between 358 and 736 MeV were considered and are listed in Table I. Of these, only 40 points were deleted from the final analysis. Thirty-eight of the deleted points are differential cross-section measurements carried out a decade or more ago, and two are spin-correlation measurements that are known from our low-energy analyses[1] to be incorrect. The final set of data included matrix representations of 588 points from about 20 to 350 MeV plus 559 data from 358 to 736 MeV. Thus a total of 1147 data are represented in the final data selection.

III. INELASTIC PARAMETRIZATIONS

The nucleon-nucleon S matrix for a given angular momentum value J has the form

$$S(J)=\begin{bmatrix} S_J & 0 & 0 & 0 \\ 0 & S_{J,J} & 0 & 0 \\ 0 & 0 & S_{J-1,J} & S^J \\ 0 & 0 & S^J & S_{J+1,J} \end{bmatrix}, \qquad (1)$$

where we use a standard notation.[2] If we consider both elastic and inelastic processes, then in an expanded Hilbert space $S(J)$ can be divided into a direct product of terms of the general form[3]

$$S=\begin{pmatrix} S_e & R \\ R^T & S_i \end{pmatrix}, \qquad (2)$$

where S_e represents elastic scattering, R gives the sum over transitions to all open inelastic channels, and S_i represents scattering between inelastic channels. S_e will be one-dimensional for the S_J and $S_{J,J}$ channels in Eq. (1), and it will be two-dimensional for the coupled channels. We assume time-reversal invariance. For the one-dimensional elastic channels, the unitarity of the S matrix leads to the familiar result

$$|S_e|^2=1-\sum_n |R^{(n)}|^2\leq 1\,, \qquad (3)$$

where the summation index n extends over all open inelastic channels having the appropriate quantum numbers. A similar set of equations holds for the coupled channels.[3]

For elastic scattering, the unitarity of the S matrix is assured by choosing matrix elements of the general form

$$S_J=e^{2i\delta_J}\,, \qquad (4)$$

with δ_J a real phase shift. When inelastic channels open up, the modulus of the scattering amplitude has an upper bound of unity, as shown in Eq. (3). The inelasticity can be represented by adding a multiplicative parameter—by adding an imaginary part to the phase shift, for example. The multiplicative factor may be chosen so that it can assume any value, in which case a least-squares search using this parameter may result in the unitarity limit being violated. Or, a form may be chosen for the inelastic parameter so that the unitarity limit shown in Eq. (3) is always maintained. The choice of parametrization is arbitrary, but we have chosen a form in which the unitarity limit cannot be exceeded. In terms of the matrix elements of Eq. (1), we use the following phase-shift forms:

$$\begin{aligned} S_J&=\cos\rho_J\, e^{2i\delta_J}\,, \\ S_{JJ}&=\cos\rho_{JJ}\, e^{2i\delta_{JJ}}\,, \\ S_{J\pm1,J}&=\cos\rho_\pm \cos2\epsilon\, e^{2i\delta_\pm}\,, \\ S^J&=i\sin2\epsilon\, e^{i(\delta_++\delta_-+\alpha)}\,. \end{aligned} \qquad (5)$$

As the inelastic threshold is approached from above, the inelastic parameters all vanish, and Eq. (5) goes over into the usual Stapp parametrization.[2]

From Eqs. (1) and (2), we can identify five kinds of transition matrices R leading to inelastic channels. We

[2] M. H. MacGregor, M. J. Moravcsik, and H. P. Stapp, Ann. Rev. Nucl. Sci. 10, 291 (1960).

[3] R. M. Arndt, Rev. Mod. Phys. 39, 710 (1967).

define the following transition amplitudes:

$$
\begin{aligned}
X_J&=\sum_n |R_J^{(n)}|^2,\\
X_{J,J}&=\sum_n |R_{J,J}^{(n)}|^2,\\
X_\pm{}^J&=\sum_n |R_{J\pm1,J}^{(n)}|^2,\\
X_0{}^J e^{i\beta}&=\sum_n R_{J-1,J}^{(n)*}R_{J+1,J}^{(n)}.
\end{aligned}
\tag{6}
$$

The relation between these quantities and the inelastic parameters ($\rho_J,\rho_{JJ},\rho_\pm,\alpha$) is given by Eq. (5) together with equations of the form of Eq. (3). We have the following:

$$
\begin{aligned}
X_J&=\sin^2\rho_J,\\
X_{JJ}&=\sin^2\rho_{JJ},\\
X_\mp{}^J&=\cos^2\epsilon\,\sin^2\rho_\mp,\\
X_0{}^J&=\sin2\epsilon\,\cos2\epsilon(\cos^2\rho_+ +\cos^2\rho_-\\
&\qquad -2\cos2\alpha\,\cos\rho_+\cos\rho_-)^{1/2},\\
\beta&=\tan^{-1}\left(\frac{C^+\sin\Delta\,\sin\alpha+C^-\cos\Delta\,\cos\alpha}{C^+\cos\Delta\,\sin\alpha-C^-\sin\Delta\,\cos\alpha}\right),
\end{aligned}
\tag{7}
$$

where

$$\Delta=\delta_+-\delta_-\quad\text{and}\quad C^\pm=\cos\rho_+\pm\cos\rho_-.$$

These quantities can be related to total reaction cross sections as follows:

$$
\begin{aligned}
\sigma_r{}^{(p,p)}&=\frac{\pi}{2k^2}\sum_{J\text{ odd}}[(2J+1)(X_{JJ}+X_+{}^J+X_-{}^J)\\
&\qquad\qquad +(2J-1)X_{J-1}],\\
\sigma_r{}^{(n,p)}&=\frac{\pi}{4k^2}\sum_J(2J+1)(X_J+X_{JJ}+X_+{}^J+X_-{}^J),
\end{aligned}
\tag{8}
$$

where k is the c.m. momentum of either nucleon.

In using inelastic data, we had two methods of procedure. One was to take a set of quantities X as given by a theoretical model, together with errors estimated to be associated with each X, and treat these as "pseudodata." They are simply added in with the data used for the least-squares sum χ^2 and serve as constraints on the inelastic parameters. Theoretical values for the set X with estimated errors were supplied to us by Amaldi[4] and used in some of our search problems, as described in the next two sections. The second method of procedure was to use measured total reaction cross sections σ_R together with Eq. (8) to serve as constraints on the inelastic parameters. This procedure is in fact the one used for our final solutions. The values for σ_R that we used are listed in Table I.

The inelastic parameter α in Eq. (5) is certainly necessary from a theoretical point of view. However, treating it as a free parameter was not particularly rewarding. The Amaldi model[4] for the inelasticity parameters gives values for the quantities X in Eq. (7), but cannot give a value for β. Thus α is only mildly constrained. The reaction cross sections from Eq. (8) do not depend on α except as coupled indirectly through the elastic phases. A search on the parameter α did result in a reduction in the least-squares sum χ^2, but α took on large and rather wildly fluctuating values. In some of the final solutions, we simply set $\alpha=0$.

It was necessary to assign some kind of energy dependence for the inelastic parameters. Since theory is of almost no help here, we used a simple expansion of the form $(T-T_0)^P$, where $T_0=400$ MeV was arbitrarily assigned as the threshold energy, and p was an exponent suitably chosen for each channel. Each inelastic parameter ρ could be represented by a sum of such terms, but in general we used only one term per inelastic parameter. In our final energy-dependent phase-shift solution, a good fit was obtained to all total reaction cross sections at 600 MeV and below. However, the fit to total reaction cross sections at 660 MeV was not very good. Thus an energy-dependent form for the inelasticity can be chosen that is better than the form we used. However, the effect on the elastic phases at 660 MeV of making slight changes in the inelasticity (particularly just in the total inelasticity) is quite small. In view of the many uncertainties that exist for other reasons at 660 MeV, we did not deem it worthwhile at this time to make further efforts to improve the treatment of the inelasticity.

IV. ENERGY-DEPENDENT PHASE-SHIFT RESULTS

An energy-dependent phase-shift analysis from 0 to 750 MeV was carried out using the data selection given in Table I. At energies above 400 MeV, the scattering amplitudes contained both an elastic and an inelastic component. In Sec. III, we have described the parametrization of the inelastic component. Although the inelastic effects must be included in order to obtain a proper treatment of the elastic effects, we could obtain little quantitative information from the present analysis about the behavior of the inelastic amplitudes. Data on inelastic reactions are meager, and the precision of the elastic scattering experiments is not yet good enough to delimit the inelastic scattering. Thus the results we present here are of interest mainly in the determinations we obtained for the elastic phases.

In our (p,p) analysis at the lower energies (paper VII), we concluded that the elastic phase-shift energy dependence labeled form A was the most advantageous one for us to use. Thus it was natural to test form A also for the higher-energy analysis. At the lower energies, we found the most meaningful solutions for form A when

[4] U. Amaldi, Jr., R. Biancastelli, and S. Francaviglia, Nuovo Cimento 47, 85 (1967); and private communication.

TABLE I. (p,p) data for 0–750 MeV analysis.

Energy (MeV)	No., type data[a]	Angular range (c.m.)	Data std. err.	Norm. std. err.	Deleted angles	M value[b]	Predict norm.[c]	Comment	Reference
25	34	Matrix representation				1.1		d	Livermore (1967)
50	99	Matrix representation				1.2		d	Livermore (1967)
95	85	Matrix representation				0.9		d	Livermore (1967)
142	183	Matrix representation				1.1		d	Livermore (1967)
210	65	Matrix representation				1.1		d	Livermore (1967)
330	122	Matrix representation				1.4		d	Livermore (1967)
358	14 C_{NN}	58°–102°	20%	9%		1.4	0.810	e	Chicago (1967A)
380	10 σ	4°–13°	~3%	Float		(4.0)	0.94	e, f, g, h, i	Liverpool (1958)
380	10 σ	14°–31°	~2%	Float		1.7	1.024	e, g	Liverpool (1958)
380	6 σ	30°–90°	1%	1.5%		0.6	0.992	e, g	Liverpool (1958)
380	1 C_{NN}	45°	50%			(32)		e, f, h	Liverpool (1966)
380	1 C_{KP}	45%	80%			(30)		e, f, h	Liverpool (1966)
382	1 C_{NN}	90°	20%			6.0		e	Liverpool (1961)
382	1 C_{KP}	90°	20%			0.3		e	Liverpool (1961)
386	14 C_{NN}	58°–101°	15%	8.6%		1.6	0.753	e	Chicago (1967A)
400	2 C_{NN}	60°–90°	60%, 15%			0.1		e	Princeton (1963)
400	2 C_{KP}	60°, 90°	75%, 30%			3.3		e	Princeton (1963)
400	7 P	33°–83°	3%	3%		1.1	0.971	e	Berkeley (1967B)
400	7 P	33°–83°	6%	3%		1.8	0.966	e	Berkeley (1967B)
415	7 P	15°–75°	5%	5.7%	90°	1.4	0.872		Carnegie (1954)
415	14 P	51°–98°	10%	4.7%		0.9	0.923		Chicago (1967A)
415	14 C_{NN}	51°–98°	15%	6.9%		1.9	0.788		Chicago (1967A)
415	1 D	90°	20%			3.2			Carnegie (1956)
419	7 σ	28°–90°	6%	10%		2.1	0.874		Chicago (1955)
425	2 D	65°–115°	3%, 7%			2.7		j	Chicago (1967B)
425	2 R	65°–115°	3%, 8%			3.6		j	Chicago (1967B)
425	2 A	65°–115°	4%, 120%			2.4		j	Chicago (1967B)
425	2 R'	65°–115°	4%, 15%			0.6		j	Chicago (1967B)
425	2 A'	65°–115°	6%, 15%			0.3		j	Chicago (1967B)
430	6 P	30°–120°	20%	10%	90°	1.5	0.880		Princeton (1965)
430	7 D	30°–120°	30%			0.7			Princeton (1965)
430	7 R	30°–120°	30%			0.5			Princeton (1965)
430	7 A	30°–120°	30%			2.2			Princeton (1965)
430	7 A'	30°–120°	50%			3.9			Princeton (1965)
431	1 σ_R		10%			1.3		k	Carnegie (1958)
437	8 σ	17°–90°	5%	5%		0.3	0.955		Carnegie (1955)
450	1 C_{NN}	90°	20%			0.5			Princeton (1963)
450	1 C_{KP}	90°	40%			1.0			Princeton (1963)
450	1 σ_R		4%			0.1		l	Chicago (1959)
460	5 σ	30°–90°	3%	10%		(4.5)	0.96	f, h, i	Dubna (1955)
460	3 σ	5°–15°	10%	Float		(4.3)	1.06	f, h, i	Dubna (1956A)
460	1 σ_R		20%			0.4			Dubna (1956A)
460	10 σ	20°–90°	5%	10%		2.2	0.970		Dubna (1954B)
460	2 σ	30°, 90°	13%, 7%			0.3			Dubna (1954C)
500	7 P	33°–82°	10%	3%		0.8	0.962		Berkeley (1967B)
500	7 P	33°–82°	8%	1.4%	64°	0.1	0.999		Berkeley (1967B)
500	23 P	34°–87°	10%	10%	90°	2.0	0.874		Saclay (1967)
510	1 σ	90°	7%			0.1			Dubna (1954C)
560	4 σ	40°–90°	5%	10%		(2.3)	1.00	f, h, i	Dubna (1955)
560	5 σ	5°–25°	10%	Float		(1.8)	1.20	f, h, i	Dubna (1956A)
560	1 σ_R		10%			0.4			Dubna (1956A)
560	1 σ_R		7%			0.5			CERN (1962)
562	2 σ	30°, 90°	10%, 6%			0.7			Dubna (1954C)
575	14 C_{NN}	36°–104°	20%	(6.1%)		1.8	0.915	m	Orsay (1966)
586	1 σ	90°	6%			3.1			Dubna (1954C)
596	16 P	23°–91°	5%			1.0		n	Orsay (1966)
600	8 P	33°–82°	10%	3%		1.0	0.994		Berkeley (1967B)
600	8 P	33°–83°	5%	3%		1.5	1.045		Berkeley (1967B)
600	1 D	67°	20%			11.8			CERN (1966)
600	1 σ_R		4%			0.3			Dubna (1967A)

TABLE I. (*Continued*).

Energy (MeV)	No., type data[a]	Angular range (c.m.)	Data std. err.	Norm. std. err.	Deleted angles	M value[b]	Predict norm.[c]	Comment	Reference
605	3 R	72°–108°	30%			3.2		o	Dubna (1967C,E)
605	1 C_{NN}	90°	80%			0.2		o, p	Dubna (1964D)
605	1 C_{KP}	90°	130%			0.1		o, p	Dubna (1964D)
605	1 C_{NN}	90°	30%			0.0		o, q	Dubna (1967B,E)
605	1 C_{KP}	90°	70%			0.3		o, q	Dubna (1967B,E)
608	5 A	54°–126°	30%			2.4			Dubna (1964A)
609	26 P	30°–90°	7%	10%		2.2	0.986		Saclay (1967)
610	2 σ	30°, 90°	9%, 6%			0.9			Dubna (1954C)
614	8 P	58°–84°	6%	19%		2.7	1.263		Berkeley (1966B)
622	1 σ	90°	7%			2.0			Dubna (1954C)
634	2 σ	30°, 90°	10%, 6%			0.9			Dubna (1954C)
635	23 P	27°–90°	3%	3.06%		0.7	1.007	o	Dubna (1967D,E)
635	2 D	47.5°, 90°	5%			1.0			Dubna (1967E)
635	10 P	27°–86°	6%	5.7%	11°, 12°, 16°, 20°, 90°	0.9	0.985	o, r	Dubna (1958)
635	5 R	54°–126°	20%			1.4			Dubna (1963A)
635	7 P	18°–68°	10%	Float	90°	0.3	0.959	s	Dubna (1964C)
635	1 D	112.5°	10%			1.7		t	Dubna (1964C)
635	5 D	54°–126°	40%			1.4		o, t, u	Dubna (1960)
640	3 C_{NN}	54°–90°	20%			2.5		o, t, u, v	Dubna (1963B)
645	2 σ	30°, 90°	10%, 6%			2.1			Dubna (1954C)
650	38 σ	6°–90°	20%	3.2%	3°	1.2	1.044	o, t, w	Dubna (1965)
650	1 σ_R		4%			39.5		o, x	Dubna (1964B)
657	2 σ	30°, 90°	9%, 6%			2.4			Dubna (1954C)
657	1 σ_R		6%			13.6		x	Dubna (1963C)
660	7 σ	30°–90°	5%	Float		4.6	1.043	o, y	Dubna (1954A)
660	7 σ	30°–90°	3%	Float		3.6	1.052	o, y	Dubna (1955)
660	5 σ	5°–25°	7%	Float		(5.8)	1.22	f, h, i, o, y	Dubna (1956A)
660	6 σ	7°–30°	6%	Float		(26.7)	1.10	f, h, i, o	Dubna (1956B)
660	1 σ_R		7%			8.3		x	Dubna (1956A)
660	1 C_{KP}	90°	70%			0.1			Dubna (1962)
667	9 P	4°–48°	10%	3%		1.5	1.075		Dubna (1966A)
679	15 P	38°–83°	3%	6.2%		2.3	1.088		Berkeley (1966B)
680	13 P	51°–89°	10%	10%		0.8	1.098		Berkeley (1967A)
680	13 C_{NN}	51°–89°	15%	10%		1.70	1.264		Berkeley (1967A)
700	8 P	29°–86°	5%	3%		1.7	1.004		Berkeley (1967B)
700	8 P	30°–86°	5%	3%		1.6	1.037		Berkeley (1967B)
735	11 P	10°–41°	4%	Float		1.6	1.123	z	Berkeley (1966A)
735	14 P	6°–74°	6%	10%		0.5	0.977		Saclay (1967)
735	15 C_{NN}	35°–92°	30%	10%		1.0	1.103		Saclay (1967)
736	17 P	32°–83°	3%	6.2%		0.8	1.010		Berkeley (1966B)

[a] The number of data shown does not include deleted points or experimentally determined normalization constants.

[b] The M value is χ^2/No. of data. The quoted M value is from the energy-dependent solution given in Table III unless otherwise noted. Deleted data sets have brackets around the M values.

[c] This is the over-all *theoretical* normalization arrived at in the final search problem. The *reciprocal* of this number gives the amount by which the experimental data should be changed to be consistent with the phase shift solution.

[d] These data were described in paper VII, and the matrices are listed there.

[e] These data were also analyzed in paper VII. [See Livermore (1967).]

[f] These data were deleted.

[g] In paper VII, these three differential cross-section measurements at 380 MeV were treated as one set of data. The entire set was deleted since it had the wrong shape. In the present work, we separated the different experimental runs, and it became apparent that only the small-angle points are incorrect and should be deleted.

[h] The M value and predicted normalization for this solution are from a preliminary analysis. These data were eliminated before obtaining the final solution.

[i] These data have the wrong shape.

[j] We are grateful to L. Pondrom for communicating these data to us in advance of publication.

[k] The value $\sigma_R = 2.43 \pm 0.25$ mb was used here, as obtained by summing over the partial cross sections given in the references and choosing an average energy.

[l] The value $\sigma_R = 3.42 \pm 0.15$ mb was used here, as obtained by summing over partial cross sections given in this reference and in the third Carnegie (1958) reference.

[m] G. Coignet (private communication) informed us that these data are absolute and should not have a normalization constant. However, we found a better fit if the data are allowed to renormalize, so we have assigned a normalization constant as shown here. Without this renormalization, the M value is 2.5.

[n] G. Coignet informed us that these data are absolute. A good fit is obtained without allowing the data to renormalize (see footnote m). We would like to thank G. Coignet for his correspondence with us.

[o] We would like to thank L. S. Azhgerei and G. D. Stoletov for sending unpublished results and comments about these data.

[p] These are older measurements and have been superseded by the data points immediately following these.

[q] These data are being refined.

[r] Renormalized values for these data were supplied to us by L. S. Azhgerei and G. D. Stoletov.

[s] We have used these data in the form quoted in Dubna (1966B), but have allowed them to normalize freely.

[t] The values used are quoted in Dubna (1966B).

[u] These data have been renormalized in connection with a new measurement of the beam polarization. See Dubna (1966A).

[v] The values at 51.2°, 54.3°, and 57.4° quoted in Dubna (1966B) are not Dubna measurements, but are actually from Berkeley (1967A). The correct value for 54° is given in Dubna (1966A).

[w] The listed reference and Dubna (1966B) both contain a few minor misprints for these data.

[x] Our forms for the inelastic phases give good fits to σ_R at 600 MeV and below, but poor fits at 650–660 MeV. More suitable forms can be chosen, but the effect on the elastic phases is not large when compared to other uncertainties existing at these energies.

[y] The original reference gives the energy as 657 MeV.

[z] It was not possible from the paper to obtain a normalization error. We floated the data since some adjustment is obviously necessary.

Table II. Data references for Table I.

Berkeley	(1966A)	Paul G. McManigal, Richard D. Eandi, Selig N. Kaplan, and Burton J. Moyer, Phys. Rev. **148**, 1280 (1966).
	(1966B)	F. Betz, J. Arens, O. Chamberlain, H. Dost, P. Grannis, M. Hansroul, L. Holloway, C. Schultz, and G. Shapiro, Phys. Rev. **148**, 1284 (1966).
	(1967A)	Helmut E. Dost, John F. Arens, Frederick W. Betz, Owen Chamberlain, Michael J. Hansroul, Leland E. Holloway, Claude H. Schultz, and Gilbert Shapiro, Phys. Rev. **153**, 1394 (1967).
	(1967B)	David Cheng, Burns MacDonald, Jerome A. Helland, and Philip M. Ogden, Phys. Rev. **163**, 1470 (1967).
Carnegie	(1954)	J. A. Kane, R. A. Stallwood, R. B. Sutton, T. H. Fields, and J. G. Fox, Phys. Rev. **95**, 1694 (1954).
	(1955)	R. B. Sutton, T. H. Fields, J. G. Fox, J. A. Kane, W. E. Mott, and R. A. Stallwood, Phys. Rev. **97**, 783 (1955).
	(1956)	J. A. Kane, R. A. Stallwood, R. B. Sutton, and J. G. Fox, Bull. Am. Phys. Soc. **1**, 9 (1956).
	(1958)	T. H. Fields, J. G. Fox, J. A. Kane, R. A. Stallwood, and R. B. Sutton, Phys. Rev. **109**, 1704 (1958); **109**, 1713 (1958); R. A. Stallwood, R. B. Sutton, T. H. Fields, J. G. Fox, and J. A. Kane, *ibid.* **109**, 1716 (1958).
Cern	(1962)	B. Baldoni, S. Focardi, H. Hromadnik, L. Monari, F. Saporetti, S. Femino, F. Mezzanares, E. Bertolini, and G. Gialanella, Nuovo Cimento **A26**, 1376 (1962).
	(1966)	M. Bourquin, E. Heer, B. Levrat, J. F. Renevey, and C. Revillard, Helv. Phys. Acta **39**, 579 (1966).
Chicago	(1955)	J. Marshall, L. Marshall, and V. A. Nedzel, Phys. Rev. **98**, 1513 (1955).
	(1959)	Lee G. Pondrom, Phys. Rev. **114**, 1623 (1959).
	(1967A)	A. Beretvas, N. E. Booth, C. Dolnick, R. J. Esterling, R. E. Hill, J. Scheid, D. Sherden, and A. Yokosawa, Rev. Mod. Phys. **39**, 536 (1967); Enrico Fermi Institute of Nuclear Studies ,University of Chicago Report No. EFINS-67-8, 410, 1967 (unpublished); and private communcation.
	(1967B)	R. Handler, S. C. Wright, L. Pondrom, P. Limon, S. Olsen, and P. Kloeppel, Phys. Rev. Letters **19**, 933 (1967).
Dubna	(1954A)	N. P. Bogachev and I. K. Vzorov, Dokl. Akad. Nauk SSSR **99**, 931 (1954).
	(1954B)	M. G. Meshcheryakov, N. P. Bogachev, B. S. Neganov, and E. V. Piskarev, Dokl. Akad. Nauk SSSR **99**, 955 (1954).
	(1954C)	M. G. Meshcheryakov, B. S. Neganov, L. M. Soroko, and I. K. Vzorov, Dokl. Akad. Nauk SSSR **99**, 959 (1954).
	(1955)	S. Ya. Nikitin, Ya. M. Selektor, E. G. Bogomolov, and S. M. Zombkovskii, Nuovo Cimento **2**, 1269 (1955).
	(1956A)	N. P. Bogachev, Dokl. Akad. Nauk SSSR **108**, 806 (1956) [English transl.: Soviet Phys.—Doklady **1**, 361 (1956)].
	(1956B)	E. S. Bogomolov, S. M. Zombovskii, S. Ya. Nikitin, and Ya. M. Selektor, in *Proceedings of the CERN Symposium on High-Energy Accelerators and Pion Physics, Geneva, 1956* (European Organization of Nuclear Research, Geneva, 1956), Vol. 2, p. 130.
Dubna	(1958)	M. G. Meshcheryakov, S. B. Nurushev, and G. D. Stoletov, Zh. Eksperim. i Teor. Fiz. **33**, 37 (1957) [English transl.: Soviet Phys.—JETP **6**, 28 (1958)].
	(1960)	Yu. P. Kumekin, M. G. Meshcheryakov, S. B. Nurushev, and G. D. Stoletov, Zh. Eksperim. i Teor. Fiz. **38**, 1451 (1960) [English transl.: Soviet Phys.—JETP **11**, 1049 (1960)].
	(1962)	V. i. Nikanorov, G. Peter, A. F. Pisarev, and Kh. Pose, Zh. Eksperim. i Teor. Fiz. **42**, 1209 (1962) [English transl.: Soviet Phys.—JETP **15**, 837 (1962)].
	(1963A)	Yu. P. Kumekin, M. G. Meshcheryakov, S. B. Nurushev, and G. D. Stoletov, Zh. Eksperim. i Teor. Fiz. **43**, 1665 (1962) [English transl.: Soviet Phys.—JETP **16**, 1175 (1963)].
	(1963B)	B. M. Golovin, V. P. Dzhelepov, R. Ya. Zulkarneyev, and Ts'ui-Wa-Ch'uan, Zh. Eksperim. i Teor. Fiz. **44**, 142 (1963) [English transl.: Soviet Phys.—JETP **17**, 98 (1963)].
	(1963C)	L. S. Azhgerei, N. P. Klepikov, Yu. P. Kumekin, M. G. Meshcheryakov, S. B. Nurushev, and G. D. Stoletov, Phys. Letters, **6**, 196 (1963).
	(1964A)	Yu. P. Kumekin, M. G. Meshcheryakov, S. B. Nurushev, and G. D. Stoletov, Zh. Eksperim. i Teor. Fiz. **46**, 50 (1963) [English transl.: Soviet Phys.—JETP **19**, 36 (1964)].
	(1964B)	V. M. Guzhavin, G. K. Kliger, Y. Z. Kolganov, A. V. Lebedev, K. S. Marish, Yu. D. Prokoshkin, V. T. Smolyankin, A. P. Sokolov, L. M. Soroko, and Ts'ui-Wa-Ch'uan, Zh. Eksperim. i Teor. Fiz. **46**, 1245 (1964) [English transl.: Soviet Phys.—JETP **19**, 847 (1964)].
	(1964C)	V. P. Dzhelepov, B. M. Golovin, V. S. Nadezhdin, and V. I. Satarov, in *Proceedings of the Twelfth Annual Conference on High-Energy Physics, Dubna, 1964* (Atomizdat, Moscow, 1965), Vol. 1, p. 11.
	(1964D)	I. Bistritsky, B. M. Golovin, R. Ya. Zulkarneyev, S. V. Medved, V. I. Nikanarov, and A. F. Pisarev, in *Proceedings of the Twelfth Annual Conference on High-Energy Physics, Dubna, 1964* (Atomizdat, Moscow, 1965), Vol. 1, p. 14.
	(1965)	V. Guzhavin, G. Kliger, V. Kolganov, A. Lebedev, K. Marish, M. Musin, Yu. Prokoshkin, V. Smolyankin, A. Sokolov, L. Soroko, and Ts'ui-Wa-ch'uan, Zh. Eksperim. i Teor. Fiz. **47**, 1228 (1964) [English transl.: Soviet Phys.—JETP **20**, 830 (1965)].
	(1966A)	L. S. Azhgereĭ, Yu. P. Kumekin, M. G. Meshcheryakov, S. B. Nurushev, V. L. Solov̌yanov, and G. D. Stoletov, Yadern. Fiz. **2**, 892 (1965) [English transl.: Soviet J. Nucl. Phys. **2**, 636 (1966)].
	(1966B)	Z. Janout, Yu. M. Kazarinov, F. Lehar, and A. F. Pisarev, Dubna Report No. E-2726, 1966 (unpublished); Yu. M. Kazarinov, F. Lehar, A. F. Pisarev, and Z. Janout, Yadern. Fiz. **5**, 140 (1967) [English transl.: Soviet J. Nucl. Phys. **5**, 97 (1967)].
	(1967A)	Yu. M. Kazarinov and Yu. N. Simonov, Yadern. Fiz. **4**, 139 (1966) [English transl.: Soviet J. Nucl. Phys. **4**, 100 (1967)].

TABLE II. (*Continued*).

	(1967B)	B. M. Golovin, R. Ya. Zulkarneyev, V. S. Kiselev, S. V. Medved, V. I. Nikanorov, A. F. Pisarev, and G. L. Semashko, Yadern. Fiz. **5**, 146 (1967) [English transl.: Soviet J. Nucl. Phys. **5**, 101 (1967)].
	(1967C)	B. M. Golovin, R. Ya. Zulkarneyev, V. S. Kiselev, S. V. Medved, V. I. Nikanorov, A. F. Pisarev, and G. L. Semashko, Dubna Report No. Pl-3167, 1967 (unpublished); Yadern. Fiz. **6**, 804 (1967) [English transl.: Soviet J. Nucl. Phys. (to be published)].
	(1967D)	V. S. Kiselev, V. S. Nadezhdin, V. I. Satarov, and R. Ya. Zulkarneyev, Dubna Report No. El-3194, 1967 (unpublished); R. Ya. Zulkarneyev, V. S. Kiselev, V. S. Nadezhdin, and V. I. Satarov, Yadern. Fiz. **6**, 995 (1967) [English transl.: Soviet J. Nucl. Phys. (to be published)].
	(1967E)	Report by Yu. M. Kazarinov, Rev. Mod. Phys. **39**, 509 (1967).
Livermore	(1967)	Paper VII by the present authors. See Ref. 1.
Liverpool	(1958)	D. Harting, J. R. Holt, and J. A. Moore, Proc. Phys. Soc. (London) **71**, 770 (1958). J. R. Holt, J. C. Kluyver, and J. A. Moore, Proc. Phys. Soc. (London) **71**, 781 (1958).
	(1961)	J. V. Allaby, A. Ashmore, A. N. Diddens, J. Eades, G. B. Huxtable, and K. Skarsvag, Proc. Phys. Soc. (London) **77**, 234 (1961).
	(1966)	J. V. Allaby, A. Chisholm, J. Eades, and A. N. James, Nucl. Phys. **77**, 449 (1966).
Orsay	(1966)	G. Coignet, D. Cronenberger, K. Kuroda, A. Michalowicz, J. C. Oliver, M. Poulet, J. Teillac, M. Borghini, and C. Ryter, Nuovo Cimento **A43**, 708 (1966).
Princeton	(1963)	E. Engels, Jr., T. Bowen, J. W. Cronin, R. L. McIlwain, and Lee G. Pondrom, Phys. Rev. **129**, 1858 (1963).
	(1965)	R. Roth, E. Engels, Jr., S. C. Wright, P. Kloeppel, R. Handler, and Lee G. Pondrom, Phys. Rev. **140**, B1533 (1965).
Saclay	(1967)	G. Cozzika, Y. Ducros, A. de Lesquen, J. Movchet, J. C. Raoul, L. van Rossum, J. Deregel, and J. M. Fontaine, Phys. Rev. **164**, 1672 (1967); reported by Y. Ducros, Rev. Mod. Phys. **39**, 531 (1967).

between 20 and 30 free parameters were used for the phase-shift fit to the data. When spanning the larger energy range 0–750 MeV, we will obviously need to use more free parameters to maintain the accuracy of the fit. In paper VII we quoted a 23-parameter form-A solution as being the most useful representation of the 0–400-MeV (p,p) scattering matrix. For the present analysis, we made form-A fits to the data using 31 and 38 free parameters.

The analysis just described is the so-called modified phase-shift analysis in which we represented the $l=0$ to $l=5$ partial waves by a form-A energy parametrization and represented the $l=6$ and higher partial waves by the one-pion-exchange (OPE) phases. Since we were now at high enough energies that the $f-h$ phases assume substantial values, it seemed to be worthwhile to push the modified analysis one step further and add in contributions from two- and three-pion exchanges as well as the OPE. It is well known that at energies below 400 MeV, the main features of both (p,p)[5] and (n,p)[6] scattering can be qualitatively represented (except for S waves) by Born amplitudes obtained from just four exchange terms—those due to the π, σ, ρ, and ω systems. To see if the high-energy parametrization would be improved by contributions from the σ, ρ, and ω resonances, we obtained matrix representations of single-energy (p,p) solutions at 25, 50, 95, 142, 210, 330, 425, and 630 MeV, and then made a fit to these matrices using just the four poles mentioned. Then, keeping these pole terms with the parameters fixed at the values we had just obtained, we added in phenomenological phases with 20 and then with 25 free parameters. The test of the usefulness of this procedure is to see if a good fit to the data can be obtained using a significantly smaller number of free parameters. The values we used for the pole parameters are the following: $g_\pi^2=15.12$, $M_\pi=135.04$ MeV, $g_\sigma^2=3.25$, $M_\sigma=450$ MeV, $g_\omega^2=2.67$, $(f/g)_\omega=0$, $M_\omega=783$ MeV, $g_\rho^2=0.35$, $(f/g)_\rho=4$, $M=763$ MeV. The masses and f/g ratios were held fixed in the initial pole fit, and only the g^2 values were allowed to vary.

Our test of energy-dependent forms for the present paper consisted of running form-A solutions with 31 and 38 free parameters, and then form-A plus σ, ω, and ρ contributions with 20 and 25 parameters. In all of these problems we used the same form for the inelasticity, namely, values fixed at 660 MeV to match the predictions of Amaldi[4] and extended to threshold (400 MeV) by the extrapolation described in Sec. III. Since the Amaldi model does not enable us to fix accurately the inelastic parameter α in Eq. (5), we ran all of these problems with α searched, with α fixed to match data at 660 MeV, and with $\alpha=0$. The results were all quite similar, and we quote values here for $\alpha=0$.

The four energy-dependent solutions in the order just mentioned above are shown in Fig. 1. The χ^2 values for these solutions are the following: (1) 31A–1568; (2) 38A–1383; (3) 20A plus poles–1785; (4) 25A plus poles–1689. These values are for a fit to representations of 1147 data. From the χ^2 values, we see at once that the addition of σ, ω, and ρ resonances did not result in any drastic improvement in the solution. In the 25A-plus-poles solution (No. 4 in Fig. 1), we have used 25 free parameters plus three adjustable g^2 values plus two f/g ratios and three masses fixed from other information plus a slight variation permitted in g_π^2, all giving a value $\chi^2=1689$. In the 31A solution, with roughly the same

[5] R. A. Arndt, R. A. Bryan, and M. H. MacGregor, Phys. Rev. **152**, 1490 (1966).
[6] R. A. Arndt, R. A. Bryan, and M. H. MacGregor, Phys. Letters **21**, 314 (1966).

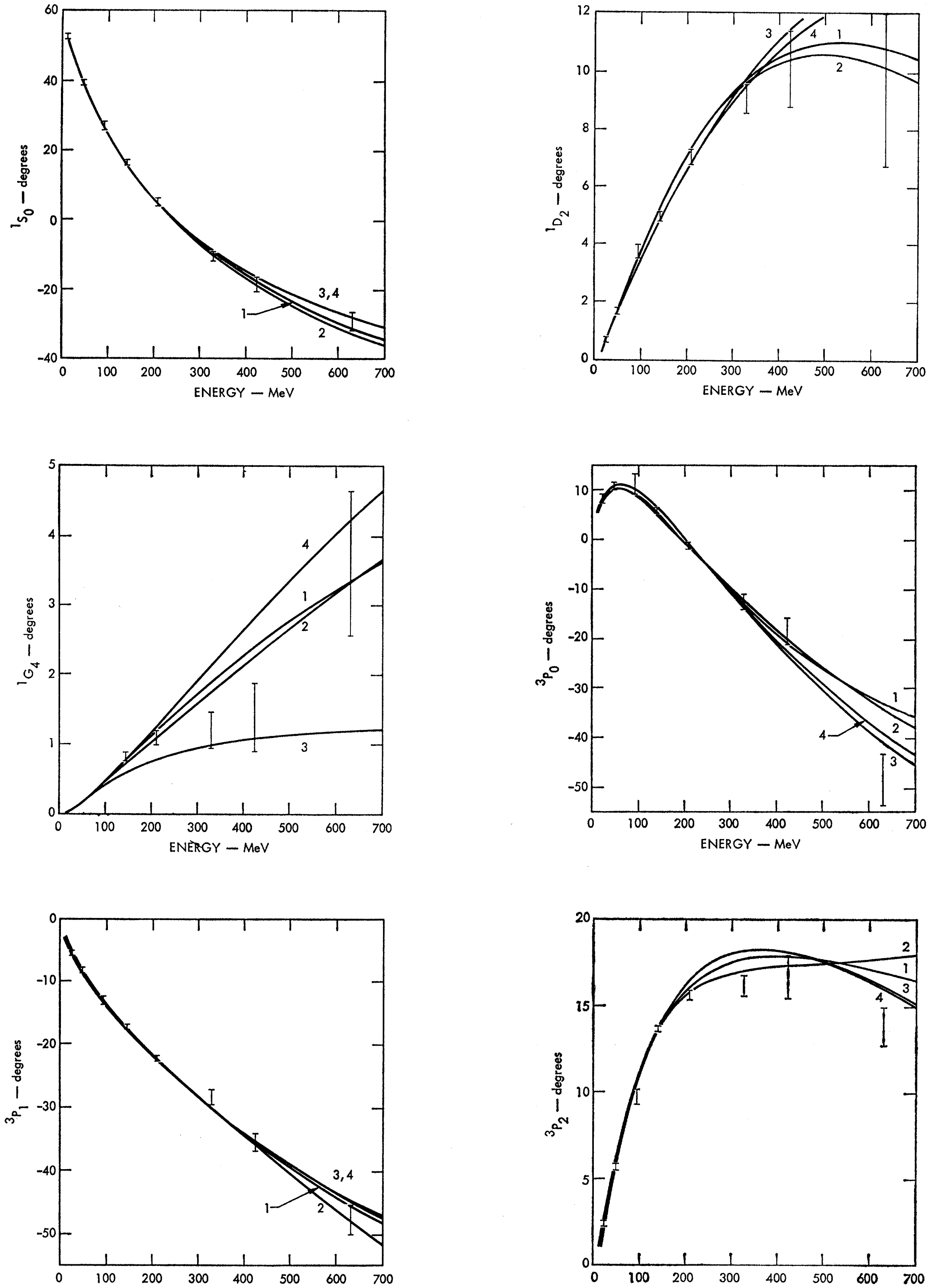

FIG. 1. Energy-dependent phase-shift solutions. The inelasticity for all of these solutions was obtained from calculations of Amaldi, as described in the text, and was held fixed. Solutions 1 and 2 are for the form-*A* energy dependence with 31 and 38 free parameters, respectively. Solutions 3 and 4 have the form-*A* energy dependence with 20 and 25 parameters, respectively, and with contributions to the phases from σ, ρ, and ω resonances added in, as described in the text. Also shown are phases as obtained from our final single-energy analyses at 25, 50, 95, 142, 210, 330, 425, and 630 MeV.

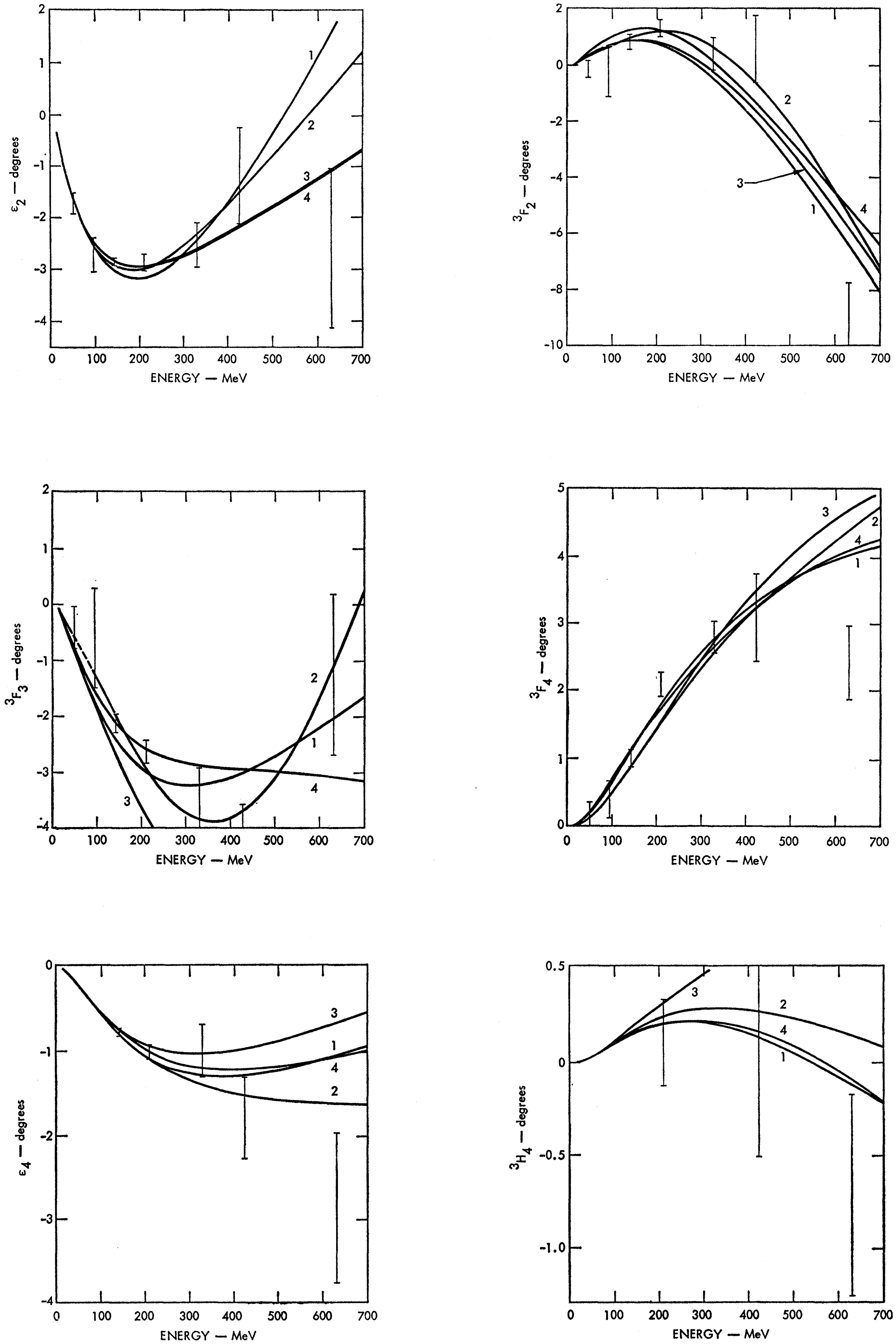

FIG. 1. (*Continued*).

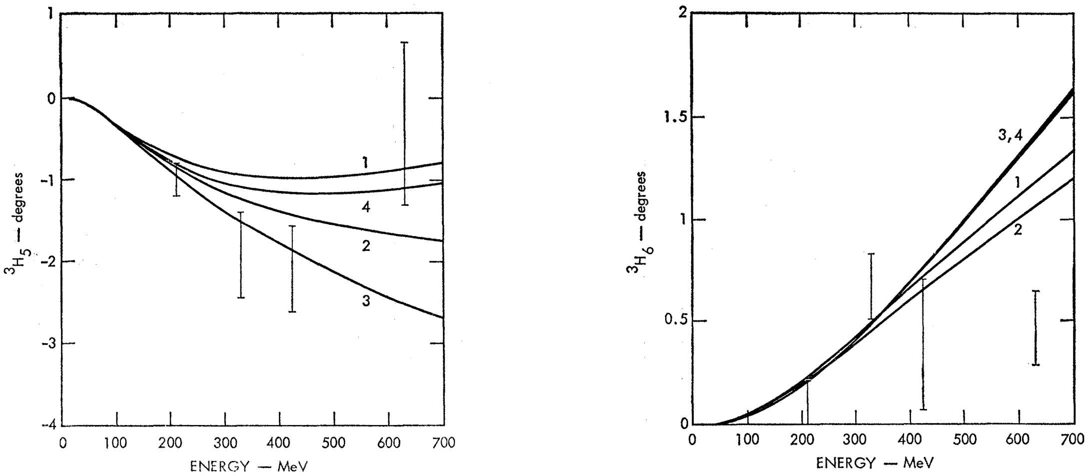

Fig. 1. (*Continued*).

amount of parameter freedom, we get $\chi^2=1568$. Thus adding in the σ, ω, and ρ contributions does not improve the analysis.

There is no clear-cut way to choose between the 31A and 38A solutions. As curves 1 and 2 in Fig. 1 show, the phases from these solutions are quite similar over most of the energy range. The χ^2 value of 1383 for 38A is somewhat lower than the value 1568 for 31A. On the other hand, it is impossible to determine if the extra wiggles allowed by the greater freedom in the 38A solution phases are really of physical significance. In paper VII, we found that 20- and 23-parameter solutions gave better high-energy extrapolations than did a 30-parameter solution. Mainly for this reason, we chose the 31A solution as the most meaningful one from the present work.

One task that still remained was to investigate the effect of varying the inelasticity. In order to give as much freedom to the inelastic phases as possible, we removed the Amaldi pseudodata that had been used in the solutions shown in Fig. 1 and replaced them with a set of total reaction cross sections σ_R. From our work with the Amaldi calculations[4] and also with single-energy analyses at 630 MeV (described in Sec. V), we concluded that the most important inelastic phases, in descending order of importance, are the following: $^1D_2$; $^3P_1$ and $^3F_3$; $^3P_2$ and $^3F_2$; $^3P_0$ and $^1G_4$. Taking the 31-parameter form-A phase-shift solution as determined above (curve 1 of Fig. 1), we ran the following choices for the inelastic phases: (1) no inelasticity; (2) $^1D_2$ inelastic; (3) $^1D_2$, $^3P_1$, $^3F_3$ inelastic; (4) $^1D_2$, $^3P_1$, $^3F_3$, $^3P_2$, $^3F_2$ inelastic; and (5) $^1D_2$, $^3P_1$, $^3F_3$, $^3P_2$, $^3F_2$, $^3P_0$, $^1G_4$ inelastic. The curves for these five solutions are given in Fig. 2. The χ^2 values for these solutions are (1) 1673 with σ_R removed, (2) 1635 with σ_R removed and 2057 with σ_R included, (3) 1575.8, (4) 1575.3, and (5) 1575.1. The σ_R data are included in (3)–(5). From these results it is apparent that some inelasticity is certainly required, even if we exclude σ_R data. On the other hand, using more than three inelastic phases gives no improvement in χ^2. However, the elastic phases do change somewhat in going from solution 3 to solution 4, as shown in Fig. 2. The elastic phases for solutions 4 and 5 are almost identical. We chose solution 4 as the most useful one from this analysis. Table III gives tabulated values for the elastic phases.

Figure 2 gives an idea of the stability of the elastic phases as the inelasticity is varied. In order to give an idea of the stability of the inelastic phases under the same variation, we show in Table IV values for the parameters ρ, as defined in Eq. (5), for solutions 2–5 of Fig. 2. We used $\alpha=0$ in all of these calculations. As can be seen in Table IV, the inelasticities obtained for solutions 3–5 are quite stable, and the inelastic phases contribute in importance in the same order that we had assigned to them. However, the present analysis really tells us little about the details of the inelastic processes. The inelastic phases that we get from a single-energy analysis at 630 MeV (described in Sec. V and shown in Table VI) exhibit a quite different splitting from the phases in Table IV.

We believe that the energy-dependent solution (31A) shown in Table III is a qualitatively correct representation of the (p,p) elastic scattering matrix from 0 to 750 MeV. A total of 1147 data is represented in the fit. The χ^2 sum is 1575, and if we remove the contributions of 61 from the σ_R data at 650–660 MeV that are not well fitted from our present inelastic forms (see Table I), we have $\chi^2=1514$. Thus $M=1.3$ for the entire elastic data set. This is statistically a very reasonable fit for this kind of analysis. And since we used the minimum parametrization that we could get by with—31 free elastic parameters—it is probable that the variations with energy of the phases given in Table III are of physical significance.

The 31A solution given in Table III has a χ^2 sum of 693 coming from the six matrix representations listed at the top of Table I. The χ^2 sum for these matrices from

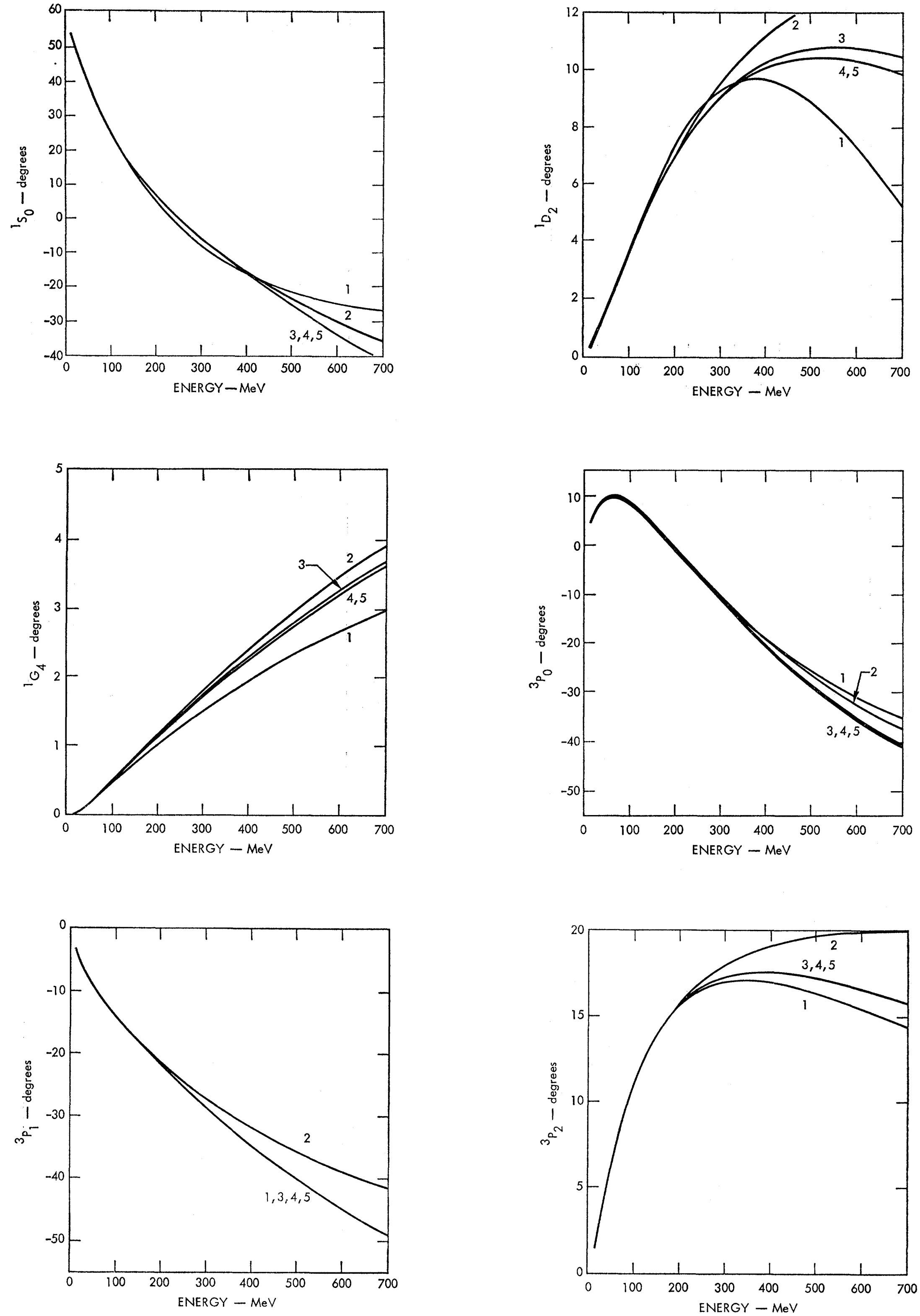

FIG. 2. The form-A 31-parameter energy-dependent solution with several choices for the inelastic parameters. The curves correspond to the following choices for free (nonzero) inelastic phases: (1) no inelasticity; (2) $^1D_2$ inelastic; (3) $^3P_1$, $^3F_3$ added; (4) $^3P_2$, $^3F_2$ added; and (5) $^3P_0$, $^1G_4$ added. Total reaction cross sections are used as constraints on the inelastic phases. Tabulated values for solution (4) are given in Table III, and values for inelasticities from solutions (2)–(5) are given in Table IV.

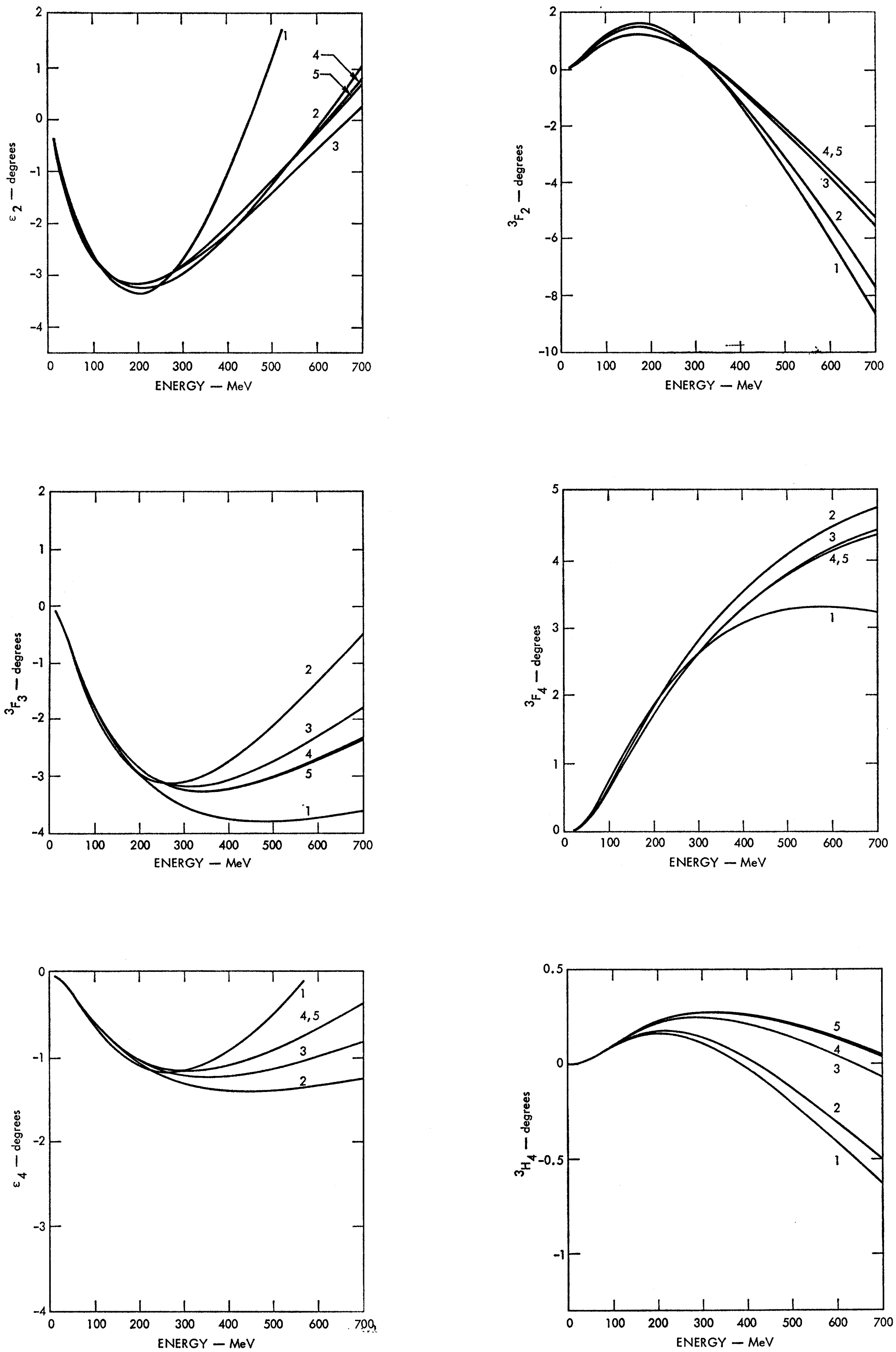

FIG. 2. (*Continued*).

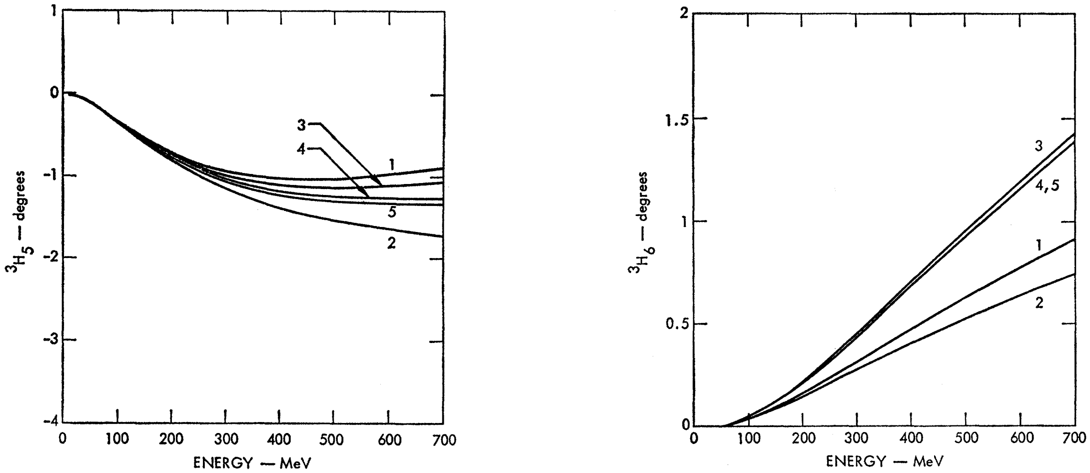

FIG. 2. (*Continued*).

the 23-parameter form-A solution of paper VII is 607. Thus the 31A solution is not quite as accurate as the 23A solution in representing the (p,p) scattering below 400 MeV. However the M value for the 31A solution is 1.2 in fitting to these low-energy data, which is a very reasonable fit. And since we use the effective-range limit for the S wave at low energies, the 31A solution will give a good fit to data below 10 MeV, even though the lowest-energy matrix used is at 25 MeV. Thus the 31A solution is a reasonable fit to the (p,p) elastic scattering data over the whole energy range 0–750 MeV. Those interested only in energies below 400 MeV can use the slightly more precise 23A solution of Table V in paper VII.

V. ENERGY-INDEPENDENT PHASE-SHIFT RESULTS

In order to complete the analysis of the high-energy (p,p) data, we carried out single-energy analyses in narrow energy bands centered at 425 and 630 MeV. This work had to be finished after completion of the

TABLE III. Energy-dependent phase-shift solution for (p,p) data from 0 to 750 MeV. Matrix representations are used for 588 data at 25, 50, 95, 142, 210, and 330 MeV, and 559 individual data from 358 to 736 MeV are treated directly. Thus a total of 1147 data are represented in the fit. $\chi^2=1575$, so that the M value (χ^2 per datum) is 1.37. A 31-parameter form-A solution is used for the energy dependence of the elastic phases, and five inelastic phases are included (this is the solution labeled 4 in Fig. 2). Only elastic phases are quoted here. Corresponding values for inelastic phases are given in solution 4 of Table IV. All elastic phases in this paper are Stapp nuclear-bar phases. The inelastic phases are defined in the text. The value $g^2=15$ is used for the pion-nucleon coupling constant.

Lab energy (MeV)	$^1S_0$	$^1D_2$	$^1G_4$	$^3P_0$	$^3P_1$	$^3P_2$	ϵ_2	$^3F_2$	$^3F_3$	$^3F_4$	ϵ_4	$^3H_4$	$^3H_5$	$^3H_4$
30	46.47	0.92	0.07	8.18	−6.15	3.62	−1.03	0.18	−0.37	0.05	−0.08	0.01	−0.03	0.00
60	35.50	2.09	0.24	10.33	−9.82	7.36	−1.94	0.54	−1.01	0.25	−0.29	0.04	−0.14	0.01
90	26.95	3.27	0.43	9.67	−12.72	10.22	−2.52	0.87	−1.59	0.54	−0.50	0.09	−0.28	0.04
120	20.05	4.41	0.62	7.67	−15.34	12.36	−2.88	1.11	−2.05	0.87	−0.69	0.13	−0.43	0.08
150	14.29	5.45	0.81	4.99	−17.79	13.95	−3.07	1.23	−2.42	1.20	−0.84	0.17	−0.56	0.12
180	9.34	6.39	1.00	1.96	−20.13	15.12	−3.16	1.25	−2.70	1.52	−0.96	0.21	−0.68	0.18
210	4.97	7.21	1.18	−1.23	−22.37	15.99	−3.15	1.19	−2.90	1.83	−1.04	0.23	−0.79	0.24
240	1.01	7.92	1.36	−4.45	−24.52	16.61	−3.08	1.04	−3.05	2.12	−1.10	0.25	−0.88	0.30
270	−2.63	8.53	1.54	−7.63	−26.59	17.04	−2.96	0.83	−3.15	2.39	−1.14	0.27	−0.96	0.37
300	−6.04	9.03	1.72	−10.75	−28.57	17.33	−2.80	0.56	−3.21	2.63	−1.15	0.27	−1.02	0.43
330	−9.27	9.45	1.89	−13.76	−30.49	17.50	−2.60	0.24	−3.24	2.86	−1.15	0.27	−1.08	0.51
360	−12.34	9.78	2.05	−16.66	−32.33	17.58	−2.38	−0.11	−3.24	3.06	−1.13	0.27	−1.12	0.58
390	−15.30	10.04	2.21	−19.43	−34.10	17.59	−2.14	−0.49	−3.22	3.25	−1.10	0.26	−1.16	0.65
420	−18.15	10.24	2.37	−22.07	−35.81	17.54	−1.89	−0.89	−3.17	3.42	−1.06	0.25	−1.19	0.72
450	−20.90	10.37	2.52	−24.58	−37.45	17.44	−1.62	−1.32	−3.12	3.58	−1.01	0.24	−1.21	0.80
480	−23.58	10.45	2.67	−26.96	−39.04	17.31	−1.34	−1.76	−3.05	3.72	−0.95	0.22	−1.23	0.87
510	−26.18	10.48	2.82	−29.22	−40.56	17.15	−1.06	−2.22	−2.97	3.85	−0.88	0.20	−1.24	0.94
540	−28.71	10.47	2.96	−31.36	−42.04	16.96	−0.77	−2.68	−2.88	3.96	−0.81	0.18	−1.25	1.02
570	−31.18	10.42	3.10	−33.38	−43.46	16.75	−0.48	−3.15	−2.78	4.07	−0.73	0.15	−1.26	1.09
600	−33.59	10.34	3.23	−35.28	−44.84	16.53	−0.18	−3.62	−2.68	4.16	−0.65	0.13	−1.26	1.16
630	−35.93	10.22	3.36	−37.08	−46.16	16.30	0.11	−4.10	−2.57	4.24	−0.56	0.10	−1.26	1.23
660	−38.23	10.08	3.48	−38.77	−47.45	16.06	0.40	−4.57	−2.46	4.32	−0.47	0.08	−1.25	1.30
690	−40.46	9.91	3.60	−40.37	−48.69	15.81	0.70	−5.05	−2.35	4.39	−0.38	0.05	−1.24	1.37
720	−42.65	9.72	3.72	−41.87	−49.89	15.56	0.99	−5.52	−2.23	4.45	−0.29	0.02	−1.23	1.43
750	−44.78	9.52	3.84	−43.27	−51.05	15.30	1.28	−6.00	−2.11	4.50	−0.19	−0.01	−1.22	1.50

TABLE IV. Inelastic phases at certain selected energies corresponding to the elastic (real) phases of Fig. 2 (solutions 2–5) and Table III (solution 4). The inelastic threshold was arbitrarily set at 400 MeV. The inelastic phases, and the forms used for their energy dependence are defined in the text.

Phase	Sol. \ Energy (MeV)	425	450	500	600	650	700	735
$^1D_2$	2	21.2	30.3	43.1	57.9	60.9	60.9	59.2
	3	17.0	24.3	34.5	46.2	48.5	48.4	46.8
	4	17.0	24.3	34.6	46.2	48.4	48.2	46.5
	5	17.1	24.4	34.6	46.2	48.3	48.0	46.2
$^3P_1$	3	7.1	11.0	18.8	36.6	47.2	59.1	68.2
	4	7.0	10.9	18.7	36.8	47.7	59.9	69.3
	5	6.9	10.8	18.6	37.1	48.2	60.8	70.5
$^3F_3$	3	6.7	10.1	15.8	26.9	32.6	38.5	42.7
	4	6.8	10.0	15.7	26.7	32.3	38.1	42.3
	5	6.6	9.9	15.6	26.5	32.0	37.8	42.0
$^3P_2$	4	0.02	0.03	0.04	0.08	0.09	0.11	0.12
	5	−0.01	−0.01	−0.01	−0.03	−0.03	−0.04	−0.04
$^3F_2$	4	0.5	0.8	1.2	2.1	2.6	3.0	3.4
	5	0.7	1.0	1.6	2.7	3.3	3.9	4.3
$^3P_0$	5	−0.1	−0.1	−0.2	−0.3	−0.4	−0.5	−0.5
$^1G_4$	5	−0.02	−0.03	−0.05	−0.09	−0.11	−0.13	−0.14

energy-dependent analysis, since we needed the phase-shift energy derivatives from the latter to properly allow for the finite spread in energies encountered in the former.

As can be seen from an inspection of Table I, the two energies mentioned above are the only regions where sufficient data exist to carry out a meaningful "single-energy" analysis. For the 425-MeV analysis, we tried two energy bands, 400–450 MeV and 415–437 MeV. At 630 MeV we also used two energy bands, 605–660 MeV and 575–680 MeV. In each case no advantage was gained by using the wider energy span. Thus the results we quote in this section are only for the narrower energy bands. All data shown in Table I between the band limits in question were used in the analyses.

At 425 MeV we first tried using an elastic analysis. This is solution 1 of Table V. Then we freed the inelastic $^1D_2$ parameter. χ^2 dropped only from 92.1 to 92.0 and the elastic phases changed hardly at all. Thus there is nothing in the (p,p) elastic scattering data at 425 MeV that *requires* us to introduce inelastic effects. This is an *a posteriori* justification for our complete neglect of inelastic effects at energies below 400 MeV. Finally, we added in the total reaction cross section deduced at 431 MeV (see Table I). Now the $^1D_2$ inelastic parameter adjusted to match this value, giving solution 2 of Table V. As can be seen, there is a slight readjustment in the elastic phases produced by the introduction of inelastic effects. This is probably the best solution we can obtain at 425 MeV. Solution 3 of Table V is the energy-dependent solution of Table III shown here for comparison purposes. The distribution of inelasticities for solution 3 is somewhat different than for solution 2, but the total reaction cross section predicted is about the same. A comparison of the elastic phases for solutions 2 and 3 shows reasonable agreement, but not always within the error limits shown for solution 2. However, on the basis of these results it seems fair to conclude that the (p,p) scattering matrix from 0 to 450 MeV is now known with fairly high precision.

TABLE V. Single-energy solutions at 425 MeV. Solution 1 has only elastic phases. Solution 2 has an inelastic component in the $^1D_2$ wave giving a fit to a total inelastic (reaction) cross section. Solution 3 is the energy-dependent solution shown here for comparison.

Solution	1	2	3 Energy-dependent solution of Table III quoted at 425 MeV
χ^2	92.1	92.9	
No. of data	95	96	
energy range (MeV)	415–437	415–437	
Real phases			
$^1S_0$	−18.73±2.00	−19.35±2.05	−18.64
$^1D_2$	10.08±1.32	10.91±1.36	10.26
$^1G_4$	1.39±0.50	1.42±0.51	2.40
$^3P_0$	−18.31±2.67	−18.19±2.68	−22.49
$^3P_1$	−35.56±1.33	−34.63±1.40	−36.09
$^3P_2$	16.69±1.23	17.18±1.30	17.53
ϵ_2	−1.20±0.93	−1.43±0.89	−1.84
$^3F_2$	0.58±1.20	0.87±1.22	−0.96
$^3F_3$	−4.10±0.54	−3.71±0.63	−3.17
$^3F_4$	3.09±0.66	3.31±0.72	3.45
ϵ_4	−1.79±0.48	−1.86±0.48	−1.05
$^3H_4$	0.06±0.57	0.08±0.59	0.25
$^3H_5$	−2.09±0.52	−2.07±0.53	−1.20
$^3H_6$	0.38±0.32	0.35±0.35	0.74
Imaginary phases			
$^1D_2$		23.46	17.03
$^3P_1$			7.0
$^3F_3$			6.8
$^3P_2$			0.0
$^3F_2$			0.5

TABLE VI. Single-energy solutions at 630 MeV. Solution 1 has predictions of inelastic phases by Amaldi, including errors, entered as data points. Solution 2 has total inelastic (reaction) cross sections in place of the Amaldi predictions. Solution 3 has inelastic phases as predicted by Amaldi, but adjusted to give a fit to total inelastic cross sections. Solution 4 was obtained by releasing the inelastic phases of solution 3. Solution 5 is the energy-dependent solution shown here for comparison.

Solution	1	2	3	4	5 Energy-dependent solution of Table III quoted at 630 MeV
No. of data	174	169	169	169	
X^2	190.8	204.8	213.5	195.7	
energy range (MeV)	605–660	605–660	605–660	605–660	
Real phases					
$^1S_0$	-29.32 ± 2.65	-20.68 ± 9.41	-32.54 ± 2.35	-35.31 ± 4.88	-35.93
$^1D_2$	9.34 ± 2.63	9.01 ± 7.17	8.59 ± 3.72	3.73 ± 5.16	10.22
$^1G_4$	3.61 ± 1.04	3.48 ± 2.45	2.38 ± 1.25	4.13 ± 2.17	3.36
$^3P_0$	-48.23 ± 5.14	-34.34 ± 8.83	-39.50 ± 6.33	-57.51 ± 12.84	-37.08
$^3P_1$	-47.74 ± 2.38	-40.20 ± 3.80	-45.77 ± 1.98	-61.25 ± 11.43	-46.16
$^3P_2$	13.75 ± 1.10	27.91 ± 2.71	18.85 ± 2.12	13.15 ± 3.48	16.30
ϵ_2	-2.59 ± 1.54	-1.13 ± 2.65	-1.79 ± 1.78	-2.92 ± 2.49	0.11
$^3F_2$	-8.87 ± 1.12	-0.23 ± 3.28	-3.30 ± 2.27	-6.50 ± 2.81	-4.10
$^3F_3$	-1.24 ± 1.44	2.99 ± 1.89	4.76 ± 1.49	-0.09 ± 2.77	-2.57
$^3F_4$	2.42 ± 0.55	4.76 ± 1.59	4.32 ± 1.02	2.91 ± 1.69	4.24
ϵ_4	-2.87 ± 0.90	-1.50 ± 1.23	-2.65 ± 1.09	-2.59 ± 1.08	-0.56
$^3H_4$	-0.72 ± 0.54	4.39 ± 0.99	0.96 ± 0.78	-0.18 ± 1.17	0.10
$^3H_5$	-0.32 ± 0.98	0.18 ± 0.95	2.44 ± 0.71	2.09 ± 1.47	-1.26
$^3H_4$	0.47 ± 0.18	2.32 ± 0.53	0.65 ± 0.26	0.53 ± 0.17	1.23
Imaginary phases					
$^1D_2$	40.0	42.6	(55.1)	37.8	47.3
$^1G_4$	10.7		(13.7)	28.7	
$^3P_0$	9.2		(11.9)	12.8	
$^3P_1$	24.6	14.1	(32.3)	54.5	43.2
$^3P_2$	15.1	34.2	(19.6)	17.0	0.1
ϵ_2	-25.6		(-25.2)	-76.0	
$^3F_2$	13.1	38.4	(16.9)	24.0	2.4
$^3F_3$	24.3	25.0	(32.3)	13.5	30.6

One interesting feature of the analysis just described is the use of some very accurate triple scattering data at 425 MeV (see Table I). These data served to considerably increase the precision of the analysis.

The situation at 630 MeV is not as favorable as that at 425 MeV, mainly because at 630 MeV the inelastic effects are quite large. We do not have a really reliable model for the inelastic contributions at 630 MeV. The Amaldi model,[4] for example, which is really supposed to be used only at energies well above 600 MeV, is off by almost a factor of 2 in its prediction for the total inelastic cross section at 630 MeV.

Several solutions at 630 MeV are presented in Table VI. The elastic data selection and the handling of the elastic phases are identical for solutions 1–4. Thus the observed differences are due mainly to the way in which the inelasticity is treated. In solution 1, the Amaldi predictions for inelastic amplitudes [the quantities X in Eq. (6) together with their estimated uncertainties] were treated as data, and the inelastic parameters were allowed to search and match these amplitudes. When we replaced the Amaldi pseudodata by total reaction cross sections and used solution 1 as a starting point, the $^1G_4$ and $^3P_0$ parameters went almost to zero, and the α parameters of Eq. (6) (reflected in ϵ_2), went to $-100°$. So we set $\alpha=0$ and put $^1G_4$ and $^3P_0$ equal to zero. Continuing the search then gave solution 2 of Table VI. Next we chose the inelastic parameters to be those predicted by Amaldi,[4] but increased them all so that they would match the known total reaction cross section. Holding them fixed and searching on the elastic parameters only gave solution 3. Then we released the inelastic parameters, with total reaction cross section data included, but with no Amaldi "data," and obtained solution 4. Solution 5 is the 31A solution of Table III quoted here for comparison.

There is no good way to choose among the solutions of Table VI. Solutions 1 and 3 are roughly on the same footing, since the inelastic phases in each case are fixed by the Amaldi constraints. Solutions 2 and 4 do not have these constraints, but differ in the number of free inelastic parameters. We obtained another solution (not shown) which had precisely the same freedom as solution 4, but which used solution 1 as a starting point (solution 4 was started from solution 3). The answers for this solution were different from those of 4 and of 2,

TABLE VII. Second-derivative matrix and error matrix for the phase-shift solution at 425 MeV (solution 2 of Table V). The units are deg^{-2} and deg^2, respectively. An imaginary phase of 23.46° should be assigned to $^1D_2$.

Second derivative matrix

	$^1S_0$	$^3P_0$	$^3P_1$	$^3P_2$	ϵ_2	$^1D_2$	$^3F_2$	$^3F_3$	$^3F_4$	ϵ_4	$^1G_4$	$^3H_4$	$^3H_5$	$^3H_6$
$^1S_0$	1.350													
$^3P_0$	−0.172	1.732												
$^3P_1$	−0.515	−0.393	1.750											
$^3P_2$	1.251	−0.488	0.270	5.847										
ϵ_2	0.014	−3.134	−0.628	−0.491	13.991									
$^1D_2$	−1.140	0.686	0.468	−1.559	0.302	4.222								
$^3F_2$	0.015	−0.333	0.623	−1.274	−4.517	−0.307	6.892							
$^3F_3$	−1.912	−3.083	−1.530	−6.736	13.745	0.259	−1.594	34.309						
$^3F_4$	−0.800	−0.058	−0.967	−4.502	0.316	−1.118	−2.036	0.580	19.994					
ϵ_4	0.544	−1.868	0.862	1.036	0.378	1.266	3.993	0.373	−5.032	13.525				
$^1G_4$	−0.867	0.476	−0.995	−0.676	0.014	−2.973	−1.251	0.493	0.909	−2.409	15.197			
$^3H_4$	0.623	−1.257	0.306	1.932	6.658	−1.179	−5.845	3.037	−3.037	−5.251	0.909	19.260		
$^3H_5$	1.567	2.650	2.245	6.157	−16.714	−2.225	4.236	−27.943	−2.880	−0.422	−2.219	−2.120	33.646	
$^3H_6$	−0.328	1.739	−0.745	1.945	0.488	1.061	−1.799	−0.838	−5.940	−1.719	0.919	−9.970	−4.499	29.656

Error matrix

	$^1S_0$	$^3P_0$	$^3P_1$	$^3P_2$	ϵ_2	$^1D_2$	$^3F_2$	$^3F_3$	$^3F_4$	ϵ_4	$^1G_4$	$^3H_4$	$^3H_5$	$^3H_6$
$^1S_0$	4.215													
$^3P_0$	1.367	7.194												
$^3P_1$	1.859	2.223	1.973											
$^3P_2$	1.290	2.360	1.043	1.702										
ϵ_2	−0.050	1.679	0.298	0.311	0.796									
$^1D_2$	2.192	0.541	0.759	1.065	−0.057	1.841								
$^3F_2$	1.050	2.449	0.860	1.277	0.528	0.829	1.480							
$^3F_3$	0.893	0.839	0.485	0.592	0.106	0.629	0.463	0.394						
$^3F_4$	0.843	1.263	0.577	0.769	0.177	0.624	0.723	0.346	0.514					
ϵ_4	−0.118	0.601	0.052	0.095	0.100	−0.094	0.143	0.047	0.132	0.229				
$^1G_4$	0.796	0.389	0.373	0.386	0.044	0.569	0.322	0.229	0.229	−0.006	0.261			
$^3H_4$	0.329	0.672	0.209	0.377	0.013	0.301	0.480	0.167	0.307	0.149	0.101	0.346		
$^3H_5$	0.239	0.253	0.007	0.061	0.225	0.255	0.123	0.184	0.108	0.034	0.097	0.030	0.279	
$^3H_6$	0.224	0.160	0.083	0.125	−0.009	0.186	0.194	0.098	0.151	0.066	0.061	0.155	0.057	0.122

although the χ^2 value was about the same. This shows the not surprising fact that when the data set is manifestly incomplete (in this case the inelastic data set), the termination point of the search can depend on the starting point, and a unique solution for a certain choice of data and of parameters may not exist. The energy-dependent solution, No. 5 in Table VI, is obtained by fitting the entire data selection, so it might be supposed to be somewhat more accurate than the other solutions. However we have no good way of assigning errors to the phases of solution 5, and without errors it is difficult to draw any meaningful conclusions.

Upon examining the individual phases listed in Table VI, it is apparent that at 630 MeV the low angular momentum phases are at least qualitatively determined, but the F waves and higher are not. This conclusion is also borne out by the high-energy behavior of the phases shown in Figs. 1 and 2. An examination of the imaginary phases in Table VI, and a comparison with the results of Table IV, reveals that we have learned little from this analysis about the actual behavior of the inelastic amplitudes. Although the various experimental groups, particularly at Dubna, have done an admirable job of improving our knowledge of the (p,p) elastic scattering data near 630 MeV, a more decisive handling of the inelasticity must be provided before we can make a satisfactory phase-shift analysis at that energy.

In Table VII we have listed the values for the second derivative matrix

$$\alpha_{l,l'}=\tfrac{1}{2}\partial^2\chi^2/\partial\delta_l\partial\delta_{l'}\,, \tag{9}$$

and for the error matrix α^{-1}, from solution 2 of Table V at 425 MeV. These matrices are for the elastic parameters only. As discussed in detail in paper VII, using these matrices is essentially equivalent to using the data directly. The second-derivative matrix is useful as a faithful representation of the data in fitting to potential models. The inverse (error) matrix is useful in calculating errors for observables and for the phase shifts themselves. The second-derivative matrix from Table VII can be used together with the six corresponding second-derivative matrices from Table VII of paper VII to provide an accurate representation of the (p,p) elastic scattering data from roughly 20 to 450 MeV. These seven matrices collectively form a representation of 684 carefully selected data that contain most of the physical content of the elastic (p,p) scattering matrix below 450 MeV. Fitting potential models to these matrices is vastly simpler than fitting to the original data, and for most purposes it is fully as accurate.

VI. CONCLUSIONS

A. Data

In a phase-shift analysis, we can only judge the correctness of a set of data by (a) comparing it with other nearby data, and (b) assuming that we have used a reasonable representation for the phase shifts. The set of 559 acceptable data between 358 and 736 MeV listed in Table I, when taken together with the low-energy data represented in the matrices listed at the top of Table I, form a set of data that reasonably meets the first requirement. The 31A phase-shift solution (Table III), which has an M value of 1.3 for the entire elastic data selection, seems to adequately fulfill the second requirement. Thus an examination of the results listed in Table I should be useful in evaluating the consistency of the data set.

The main point that seems to emerge from a study of Table I is that when a polarized target is used, there is considerable difficulty in determining the over-all normalization factor. Our analysis indicates that the experimental Chicago C_{NN} values at 358, 386, and 415 MeV are too low by about 20%, which is 2 or 3 times the quoted uncertainty in the over-all normalization. This would seem to indicate that the effective target polarization was not as large as it was thought to be. This same remark applies, although to a lesser extent, to the Chicago polarization measurements at 415 MeV, the Saclay polarization measurements at 500 MeV, and the Orsay C_{NN} measurements at 575 MeV. In each case the experimental values seem to be about 10% low. On the other hand, the Berkeley measurements of polarization at 614 MeV and of C_{NN} at 680 MeV seem to be too large by some 26%.

The Berkeley polarization measurements at 700 MeV differ in normalization from the Dubna and Berkeley polarization values at 667, 679, and 680 MeV by about 8%. However, these variations are all reasonably in agreement with the quoted uncertainties in the normalization constants. There is also some variation in the normalizations shown for data at 735 and 736 MeV, although since this is at the limit of our energy range, we can say nothing definitive about the normalizations here. The CERN measurement of D at 600 MeV does not appear to be correct.

Although a rather complete set of elastic scattering data exists near 630 MeV, more information about the inelastic scattering is required before a really meaningful phase-shift analysis can be carried out, as described in Sec. V. Triple scattering measurements with an accuracy of 5%, such as those recently carried out by the Chicago and Wisconsin groups at 425 MeV and by the Dubna group at 635 MeV, are of considerable help in sharpening the precision of the phase-shift analysis. The experimental situation in the 450–600-MeV energy range and at energies above 700 MeV is still pretty bleak, although we may hope for rapid improvement in some areas in the near future.

B. Elastic Scattering

This has been reasonably well summarized in the preceding sections. The (p,p) elastic scattering matrix is quite accurately determined by the data over the whole energy range 0–450 MeV. Above 450 MeV, inelastic effects become important, and a really accurate analysis is not yet possible. The form-A solution with 23 parameters, as quoted in Table V of paper VII, gives a precision fit to the (p,p) data from about 2 to 400 MeV. The form-A solution with 31 free elastic parameters, as quoted in Table III of the present paper, gives an accurate fit to the (p,p) elastic scattering data from 2 to 736 MeV. The value of M, the χ^2 average per data point, is about 1.3 over this whole span of energies.

The fact that the form-A solution, with only 31 free parameters, can give a good representation of the (p,p) elastic phases from threshold all the way to 750 MeV is really quite remarkable. That this economy of parametrization is possible presumably comes from the fact that we have insisted that our energy-dependent forms have a threshold behavior and a singularity structure consistent with the requirements of analyticity and unitarity. Some work has been done in investigating this statement,[7,8] but it is an area in which further investigation may be rewarding.

Our use of well-defined mathematical forms to represent the phase-shift energy dependence is of paramount importance from the standpoint of carrying out an accurate phase-shift analysis. Since the phase-shift parameters are well defined mathematically, we can use a matrix search in which all parameters are varied simultaneously in a correlated fashion.[9] One of the products of the matrix search is a second-derivative parameter matrix that, together with its inverse, contains the entire information content about the statistical errors in the analysis. These matrices can be used to print out corridors of errors for the energy-dependent phase shifts, to predict observables with errors, to handle the data normalization constants in a rigorous manner (the so-called reduced matrix representations[9]), and to generate matrix representations for all or a portion of the data. Without the extensive use of matrix techniques, the various systematic parameter studies that we have described in paper VII and in the present paper would have required a prohibitive amount of computer time. The matrix search method is indispensible for accurately arriving at a minimum in a multidimensional parameter space and for evaluating the statistical significance of the minimum once it has been reached.

---

[7] M. H. MacGregor, Phys. Rev. Letters **12**, 403 (1964).

[8] R. A. Arndt and M. J. Moravcsik, Nuovo Cimento **A51**, 108 (1967).

[9] R. A. Arndt and M. H. MacGregor, *Methods in Computational Physics* (Academic Press Inc., New York, 1966), Vol. 6, p. 553.

C. Inelastic Scattering

The results obtained in the present paper clearly illustrate that inelastic effects are of importance above 400 MeV, and also that the way in which the inelastic scattering is handled affects the results obtained for the elastic scattering in a nontrivial manner. Unfortunately, the process in which two nucleons scatter inelastically and produce a pion is a complicated problem from a theoretical point of view. No satisfactory treatment of this problem has yet been carried out. Also, the experimental data are still very meager.

Most of the theoretical approaches to this problem have centered around the viewpoint, first set forth in calculations by Mandelstam,[10] that the final-state interaction is dominated at low energies by the formation of a (3,3) resonance between the outgoing pion and one of the nucleons. This approach does not really constitute a dynamical model at present, but it merely gives an estimate based on angular momentum considerations as to which nucleon-nucleon phases are likely to be inelastic near threshold.

In the previous (p,p) analyses at 660 MeV by groups from Dubna[11] and Kyoto,[12] the Mandelstam model was used to guess which phase shifts should be given inelastic parts. The inelastic phases were then simply freed, either singly or in simple combinations, and allowed to adjust to measured reaction cross sections in a conventional χ^2 minimization search problem. This is essentially the approach that we used for solutions 2 and 4 of Table VI.

In the present paper we have tried to carry this approach one step further by using a theoretical calculation, supplied to us by the Rome group[4,13] that predicts matrix elements for the scattering to the various inelastic channels. However this model was designed to explain scattering processes at energies in the BeV region, and its use at an energy as low as 630 MeV is open to question, even if we assume that it constitutes a valid calculation at the higher energies. The total reaction cross section predicted by this model is too low by about a factor of 2 at energies around 600 MeV. However, it may be that the ratios of the inelastic matrix elements as calculated from the model have some significance at 630 MeV. If this is true, then solution 3 of Table VI should be approximately correct, since here we have kept the Amaldi ratios but adjusted the over-all normalization to match the correct total reaction cross section.

Since we have no way of judging the accuracy of the Amaldi model,[4] the only conclusion we can draw from Table VI is that the way the inelasticity is handled does make a sizeable difference in the answers obtained for the elastic phases. This being the case, a really accurate phase-shift analysis at 630 MeV must be deferred until a more decisive treatment of the inelasticity is possible.

[10] S. Mandelstam, Proc. Roy. Soc. (London) **A244**, 491 (1958).
[11] See, e.g., Yu. M. Kazarinov, Rev. Mod. Phys. **39**, 706 (1967).
[12] See, e.g., N. Hoshizaki, Rev. Mod. Phys. **39**, 700 (1967).
[13] U. Amaldi, Jr., Rev. Mod. Phys. **39**, 649 (1967).

ACKNOWLEDGMENTS

The present analysis would not have been possible without the spirited cooperation of experimentalists all over the world, who sent us data in advance of publication and who discussed with us the many details associated with the proper handling of the data. In the footnotes to Table I, we tried to acknowledge some of the communications. In addition to the workers mentioned there, conversations and correspondence with the following people were very helpful: D. Cheng from Berkeley; N. Booth and A. Beretvas from Chicago; Yu. Kazarinov, L. Lapidus, and M. Meshcheryakov from Dubna; A. Ashmore from London; and P. Catillon, Y. Ducros; L. Van Rossum, and others from Saclay. L. Pondrom aided our analysis considerably by supplying data to us verbally the same day it was measured. Our theoretical analysis was furthered by conversations and correspondence with U. Amaldi from Rome, who supplied us with the model calculations described in the paper, and with N. Hoshizaki from Kyoto and Yu. Kazarinov from Dubna. Finally, we would like to thank S. Fernbach for his support of this work at Livermore.